

## DNA-loop extruding condensin complexes can traverse one another

Kim, Eugene; Kerssemakers, Jacob; Shaltiel, Indra A.; Haering, Christian H.; Dekker, Cees

**DOI**

[10.1038/s41586-020-2067-5](https://doi.org/10.1038/s41586-020-2067-5)

**Publication date**

2020

**Document Version**

Accepted author manuscript

**Published in**

Nature

**Citation (APA)**

Kim, E., Kerssemakers, J., Shaltiel, I. A., Haering, C. H., & Dekker, C. (2020). DNA-loop extruding condensin complexes can traverse one another. *Nature*, 579(7799), 438-442.  
<https://doi.org/10.1038/s41586-020-2067-5>

**Important note**

To cite this publication, please use the final published version (if applicable).  
Please check the document version above.

**Copyright**

Other than for strictly personal use, it is not permitted to download, forward or distribute the text or part of it, without the consent of the author(s) and/or copyright holder(s), unless the work is under an open content license such as Creative Commons.

**Takedown policy**

Please contact us and provide details if you believe this document breaches copyrights.  
We will remove access to the work immediately and investigate your claim.

# **DNA-loop extruding condensin complexes can traverse one another**

Eugene Kim<sup>1</sup>, Jacob Kerssemakers<sup>1</sup>, Indra A. Shaltiel<sup>2</sup>, Christian H. Haering<sup>2</sup>, Cees Dekker<sup>1,\*</sup>

<sup>1</sup>Department of Bionanoscience, Kavli Institute of Nanoscience Delft, Delft University of Technology, Delft, Netherlands.

<sup>2</sup>Cell Biology and Biophysics Unit, Structural and Computational Biology Unit, European Molecular Biology Laboratory (EMBL), Heidelberg, Germany.

\*Correspondence to C.Dekker@tudelft.nl

**Condensin, a key member of the Structure Maintenance of Chromosome (SMC) protein complexes, has recently been shown to be a motor that extrudes loops of DNA<sup>1</sup>. It remains unclear, however, how condensin complexes work together to collectively package DNA into chromosomes. Here, we use time-lapse single-molecule visualization to study mutual interactions between two DNA-loop-extruding yeast condensins. We find that these one-side-pulling motor proteins are able to dynamically change each other's DNA loop sizes, even when located large distances apart. When coming into close proximity, condensin complexes are, surprisingly, able to traverse each other and form a new type of loop structure, which we term Z-loop – three double-stranded DNA helices aligned in parallel with one condensin at each edge. Z-loops can fill gaps left by single loops and can form symmetric dimer motors that reel in DNA from both sides. These new findings indicate that condensin may achieve chromosomal compaction using a variety of looping structures.**

The spatial organization of chromosomes is critical to life at the cellular level. Structural Maintenance of Chromosomes (SMC) complexes including condensin, cohesin, and the Smc5/6 complex are key players for DNA organization in all organisms<sup>2-5</sup>. An increasing amount of evidence suggests that the underlying principle of DNA organization by SMC complexes is to actively create and enlarge loops of DNA, a process named loop extrusion<sup>6</sup>. Polymer simulations<sup>7,8</sup> and chromosome conformation capture (Hi-C) data on topologically associating domains<sup>9-12</sup> suggested the formation of such DNA loops, while recent *in vitro* single-molecule studies provided clear experimental evidence of condensin's DNA translocase activity<sup>13</sup> and its ability to extrude loops of DNA<sup>1</sup>.

It remains to be seen how DNA loop extrusion by individual condensins relates to the condensation of DNA into mitotic chromosomes. Current modelling has so far assumed that translocating SMC complexes block when they collide, resulting in a string of loops clamped together at their stems by adjacent condensins<sup>9,12</sup>. Recent polymer simulations<sup>14</sup>, however, showed that this assumption fails to explain the high degree of compaction observed in mitotic chromosomes<sup>15</sup> if considering asymmetric extrusion of loops by condensin, the property found in *in vitro* experiments<sup>1</sup>. Experimental evidences for both condensin<sup>16</sup> and cohesin<sup>17-20</sup>, suggested mutual interactions and a close spacing of SMC proteins<sup>21</sup>. Here, we study the cooperative action of condensin complexes by time-lapse single-molecule visualization. The data reveal a set of distinct interactions between DNA loop-extruding condensins, including the re-shuffling of individual loop sizes and the striking ability of condensins to traverse one another to form a dimeric motor that reels in DNA from both sides and creates a novel type of condensed DNA.

To study the interaction between multiple condensin-mediated DNA loops, we imaged the extrusion of DNA loops by budding yeast condensin on 48.5-kilobasepair (kbp)  $\lambda$ -DNA substrates that were tethered at both ends to a passivated surface and stained with Sytox orange<sup>1</sup> (SxO) (Fig. 1a). Upon addition of condensin and ATP, we observed DNA loops as bright fluorescent spots (Fig. 1b), which could be stretched into loops by applying an inplane buffer flow perpendicular to the attached DNA. While our previous study<sup>1</sup> focused on the properties of single loops at a protein concentration of 1 nM, we here explored slightly higher concentrations (2–10 nM). Notably, such concentrations, at which we observe a few condensins binding per DNA molecule (on average 1 condensin per 12 $\pm$ 4 kbp, measured at 4 nM;  $n=10$ ; Methods), approach the *in vivo* situation in the yeast nucleus, where a rough estimate (Supplementary Information) indicates 1 condensin per ~10 kbp of DNA<sup>22,23</sup>.

We first consider the case where two condensins bound at different positions along the same DNA molecule and subsequently extruded individual loops. In this case, we observed two locally compacted DNA regions, which could be stretched into loops under buffer flow (Fig. 1c). Since yeast condensin extrudes DNA loops asymmetrically<sup>1</sup>, where the side from which DNA is reeled into the loop is presumably set by the orientation of the Ycg1/Brn1 DNA-anchor site<sup>1,24</sup>, two individual DNA loops

either maintain a finite gap between them (Fig. 1d, Extended Data Fig. 1a,b) or converge towards each other (Fig. 1e). We observed a 25:75% distribution of mutually non-converging or converging loops (Fig. 1f). This ratio perfectly agrees with the expected distribution for a random orientation of two condensins, given that only one out of four possible orientations of two condensins (anchor sites facing towards each other) should produce non-converging loops.

Unexpectedly, we found that loops can influence each other, even if separated far apart. Upon initiation of a second loop, the pre-existing loop often began to shrink (70% of cases;  $n = 40$ ) (Fig. 1g, Supplementary Video 1, Extended Data Fig. 1c,d). The changes in DNA length of the two loops exhibited a clear anticorrelation (Fig. 1h, 1i, and Extended Data Fig. 1e), showing that the new DNA loop extruded by the second condensin grew at the expense of the original one. Loop shrinkage was more pronounced at higher DNA tension (Extended Data Fig. 1f) and could also be solely induced by increasing the tension by applying a larger buffer flow (Extended Data Fig. 2a-c, Supplementary Video 2). These results show that DNA in a loop can slip back through the condensin, caused by an increase in DNA tension that occurs as a second condensin starts reeling in DNA. Notably, loop slippage occurred mostly from the non-anchor site of condensin (Extended Data Fig. 2a-c, Supplementary Video 2), while at higher ionic strength conditions (e.g. 125 mM NaCl, 5 mM MgCl<sub>2</sub>), where the strength of condensin's DNA anchor is reduced,<sup>1</sup> it occurred from both sides of condensin (Extended Data Fig. 2d-g). The finding that loop extrusion of a remotely located condensin on the same DNA substrate can induce shrinkage of an already extruded loop implicates that it is possible to redistribute individual DNA loop sizes (Fig. 1j).

Surprisingly, separate individual loops were *not* the majority class of DNA structures in the experiments with higher condensin concentrations. Instead of individual parallel loops, we predominantly observed a higher-order DNA structure that appeared as an elongated line of high fluorescence intensity with a single condensin located at both edges (Fig. 2a, b, Extended Data 3 for quantification). Imaging under a sideways flow revealed that the observed structure consisted of three dsDNA stretches connected in parallel (Fig. 2b, Extended Data Fig. 4 and Supplementary Video 3). We name this structure a *Z-loop*, since its shape resembles the letter Z. The probability to observe *Z*-loops increased with the condensin concentration and became the majority pattern for concentrations higher than 6 nM (Fig. 2c). Similar data were obtained at physiological salt concentrations (125 mM NaCl, 5 mM MgCl<sub>2</sub>, 10 nM condensin, Extended Data Fig. 5a).

Real-time imaging of the flow-stretched DNA revealed the characteristic formation of a *Z*-loop (Fig. 2d, Supplementary Video 4, Extended Data Fig. 6): After a single loop had been extruded, a locally compacted region – presumably a small loop formed by an additional condensin – appeared within the initial loop (453 s) and approached to the stem of the single loop (459 s). This ‘nested loop’ of two smaller parallel loops did not stop at this point, but instead began to extend towards the DNA outside

of the initial loop (540 s) and continued to stretch until it either hit the tethered end of DNA (629 s) or until the motion stalled, presumably due to the tension in the DNA. To trace the position of the two condensins during Z-loop formation, we co-imaged DNA and condensin labelled with a single fluorophore (ATTO647N) (Fig. 2f and Supplementary Video 5, Extended Data Fig. 7). This revealed that after some time  $\Delta t_1$  after the initiation of the first loop, an additional condensin bound to a position within the initial DNA loop (59 s) and subsequently approached the stem of the loop (63 s), where the first condensin was located. After a brief waiting time  $\Delta t_2$ , one of these condensins then moved away from the stem of the loop and translocated along the DNA outside of the loop, resulting in a Z-loop (92 s). To identify which of the two condensins co-localized at the ‘leading edge’ of the Z-loop, we examined events where the first condensin had photobleached before the binding of the second condensin (Fig. 2f, Extended Data Fig. 8, Supplementary Video 6). These experiments unambiguously show that it was the second condensin that, strikingly, traversed the first condensin at the base of the first DNA loop.

We then quantified the data. The initial lag time  $\Delta t_1$ , the interval between the start of the initial loop extrusion and the start of the loop-within-a-loop formation, decreased with protein concentration (Fig. 2g), as expected, since it should correlate with the time lag between binding events of the first and second condensin. The second lag time  $\Delta t_2$ , the interval between the end of the formation process of a loop within a loop (i.e. when the second condensin reached the first one) and the start of Z-loop formation was short ( $7 \pm 6$  s) and independent of protein concentration. This quantifies the time that two condensins spent in close proximity to each other before the second condensin traversed the first one. The DNA-loop expansion rate (Fig. 2h, Methods) was similar for single loops and loops within loops ( $0.7 \pm 0.4$  kbp/s and  $0.9 \pm 0.3$  kbp/s, respectively), consistent with the notion that the observed compaction of the single loop is induced by a second condensin reeling in, at the same speed, a loop within the initial loop. The observed rate of Z-loop formation was lower ( $0.1 \pm 0.1$  kbp/s), likely due to the high tension in the DNA tether after the full extrusion of a single loop ( $\sim 0.4$  pN). Indeed, at high tensions, the average rates of single loop and Z-loop formation were similarly low (Extended Data Fig. 9g). To compare single- and Z-loop formation at low tension, we measured their respective rates in a single-tethered assay where only one end of the DNA was attached to the surface and DNA was flow-stretched (Extended Data Fig. 10a,b). This yielded speeds of  $0.8 \pm 0.4$  kbp/s and  $1.3 \pm 0.6$  kbp/s, respectively, i.e., a speed of Z-loop formation that was in fact higher than that for single loops. Once formed, Z-loops were even more stable than single loops (Extended Data Fig. 5b,c).

Z-loops also formed when two separate loops formed individually on the DNA tether and mutually collided (Fig. 2i, Extended Data Fig. 6d, Supplementary Video 7). However, in our double-tethered DNA assay, these events were rare ( $\sim 7\%$ ), largely because the increase in DNA tension during loop formation often stalled the two condensin motors before they would merge, whereas these events

129 occurred more frequently in our single-tethered DNA assay, where the DNA continually exhibits a  
130 low tension. Thus, the double-tethered assay favors Z-loop formation by binding of the second  
131 condensin within the loop formed by the first one, since the DNA within that loop is not under tension.

132 Our data reveal the characteristic pathway of two condensins that traverse each other and, as a result,  
133 form a Z-loop (Fig. 3a). Upon forming a loop within a loop, the second condensin approaches the first  
134 condensin, shortly pauses ( $\Delta t_2 \sim 7$  s), and then reaches out to the *trans* DNA outside of the first loop.  
135 Here, regardless of the two possible relative orientations of two condensins (zoomed images in Fig.  
136 3a), the second condensin can in principle reach out to the DNA next to the anchor site or to the site  
137 opposite to the anchor of the first condensin (route I or II, respectively). After the direction is chosen,  
138 the second condensin traverses the first condensin and translocates along the DNA, forming a three-  
139 stranded Z-loop. Interestingly, these two routes I and II lead to qualitatively different loops, viz., a Z-  
140 loop that reels in DNA from both sides (top) or only from one side (bottom). By comparing the  
141 relative direction of single-loop growth before stalling and the direction of subsequent Z-loop  
142 extension (Fig. 3b), we, surprisingly, did not observe a 50:50% distribution of both types, as could be  
143 expected for random relative orientations of the two condensins, but rather a 75:25% distribution of  
144 two-side-pulling verses one-side-pulling Z-loops (Fig. 3c). The observed strong bias to form two-side-  
145 pulling Z-loops likely originates from a preference for the second condensin to traverse to DNA  
146 beyond the anchor site of the first condensin (route I). In the (rare) cases that a Z-loop initiated very  
147 early (i.e. for small  $\Delta t_1$ ) and thus the second condensin bound within the initial loop before the first  
148 condensin was stalled, we observed that the Z-loop expanded symmetrically to both directions,  
149 directly confirming two-side pulling (Fig. 3d, Supplementary Video 9). Two-side pulling was  
150 observed more frequently in single-tethered DNA where the DNA substrate was under low tension  
151 (Fig. 3e, Extended Data Fig. 10b). For double-tethered DNA, once Z-loops were fully extended, they  
152 occasionally (~30%) slipped DNA from one or both of the edges, leading to random diffusion along  
153 the DNA tether over time (Extended Data Fig. 10h). Remarkably, the data show that condensin, which  
154 individually is a one-side pulling motor, can cooperatively reel in DNA from both sides in the form of  
155 a two-side pulling Z-loop driven by a condensin dimer.

156 These discoveries of interactions between DNA-loop extruding condensin complexes have important  
157 implications for understanding the fundamental mechanisms of chromosome organization. The finding  
158 that multiple DNA loops can change their sizes via slippage adds valuable information to the current  
159 picture of loop-extrusion dynamics, which so far only considered the formation, growth, and  
160 dissociation of loops. Whereas our previous discovery of an asymmetry of DNA-loop extrusion posed  
161 a problem, since this mechanism would leave gaps in-between loops<sup>14</sup>, the newly discovered Z-loops  
162 may extend along the unextruded parts of DNA, thereby filling such gaps (e.g. Fig. 3f, top, and  
163 Supplementary Video 10). Notably, in this case, a Z-loop does not reduce the DNA end-to-end length

more than two individual loops (Extended Data Fig. 10c-g), but it rather changes its topology into a more condensed Z structure. If Z-loops initiate rapidly after the nucleation of single loops, they result in two condensins anchored close to each other that frequently yield a two-side-pulling condensin dimer that reels in DNA symmetrically (Fig. 3g, bottom). Notably, in this case, the resulting extruded loop is split into two loops, contrary to the common view of a single loop being extruded. Rather than individual parallel loops, Z-loops might be the norm, given their frequent occurrence. Most importantly, the unanticipated ability of condensin complexes to traverse one another has direct consequences for modeling of chromosomes<sup>8,11</sup>. This transit of the condensin barrier may constitute a special case of a more general phenomenon of obstacle bypassing by SMCs<sup>25,26</sup>. Models of chromosome compaction will need to consider these findings that SMC proteins exhibit the ability to form a rich variety of looping structures.

**Acknowledgments:** We thank S. Bravo, J. van der Torre, and E. van der Sluis for technical support, and J. Eeftens, M. Ganji, A. Katan, B. Pradhan, B. Rowland, J.-K. Ryu, and J. van der Torre for discussions.

**Funding:** This work was supported by the Marie Skłodowska-Curie individual fellowship (to E.K.), the ERC grants SynDiv 669598 (to C.D.) and CondStruct 681365 (to C.H.H.), the Netherlands Organization for Scientific Research (NWO/OCW) as part of the Frontiers of Nanoscience and Basyc programs, and the European Molecular Biology Laboratory (EMBL).

**Author contributions:** E. K. and C. D. designed the single-molecule visualization assay, E. K. performed the imaging experiments, J. K. contributed in image analyses, I. A. S. developed condensin fluorescence labeling strategies and purified protein complexes, C. D. and C. H. H. supervised the work, all authors wrote the manuscript.

**Competing interests:** All authors declare that they have no competing interests.

**Data and materials availability:** Original imaging data and protein expression constructs are available upon request. The Matlab source code used for quantification of the number of condensins and the amount of DNA sizes is available at [https://github.com/jacobkers/BN\\_CD18\\_EK\\_CondensinTrack](https://github.com/jacobkers/BN_CD18_EK_CondensinTrack).



## References

1. Ganji, M. *et al.* Real-time imaging of DNA loop extrusion by condensin. *Science* (80-. ). **360**, 102–105 (2018).
2. Uhlmann, F. SMC complexes: From DNA to chromosomes. *Nat. Rev. Mol. Cell Biol.* **17**, 399–412 (2016).
3. Hassler, M., Shaltiel, I. A. & Haering, C. H. Towards a Unified Model of SMC Complex Function. *Curr. Biol.* **28**, R1266–R1281 (2018).
4. van Ruiten, M. S. & Rowland, B. D. SMC Complexes: Universal DNA Looping Machines with Distinct Regulators. *Trends Genet.* **34**, 477–487 (2018).
5. Nolivos, S. & Sherratt, D. The bacterial chromosome: Architecture and action of bacterial SMC and SMC-like complexes. *FEMS Microbiol. Rev.* **38**, 380–392 (2014).
6. Nasmyth, K. Disseminating the Genome: Joining, Resolving, and Separating Sister Chromatids During Mitosis and Meiosis. *Annu. Rev. Genet.* **35**, 673–745 (2001).
7. Alipour, E. & Marko, J. F. Self-organization of domain structures by DNA-loop-extruding enzymes. *Nucleic Acids Res.* **40**, 11202–11212 (2012).
8. Goloborodko, A., Imakaev, M. V., Marko, J. F. & Mirny, L. Compaction and segregation of sister chromatids via active loop extrusion. *Elife* **5**, 1–16 (2016).
9. Naumova, N. *et al.* Organization of the Mitotic Chromosome. *Science* (80-. ). **342**, 948 LP – 953 (2013).
10. Sanborn, A. L. *et al.* Chromatin extrusion explains key features of loop and domain formation in wild-type and engineered genomes. *Proc. Natl. Acad. Sci.* **112**, E6456–E6465 (2015).
11. Fudenberg, G. *et al.* Formation of Chromosomal Domains by Loop Extrusion. *Cell Rep.* **15**, 2038–2049 (2016).
12. Gibcus, J. H. *et al.* A pathway for mitotic chromosome formation. *Science* (80-. ). **359**, eaao6135 (2018).
13. Terakawa, T. *et al.* The condensin complex is a mechanochemical motor that translocates along DNA. *Science* (80-. ). **358**, 672–676 (2017).
14. Banigan, E. J. & Mirny, L. A. Limits of Chromosome Compaction by Loop-Extruding Motors. *Phys. Rev. X* **9**, 31007 (2019).
15. Paulson, J. R. & Laemmli, U. K. The structure of histone-depleted metaphase chromosomes. *Cell* **12**, 817–828 (1977).
16. Keenholtz, R. A. *et al.* Oligomerization and ATP stimulate condensin-mediated DNA compaction. *Sci. Rep.* **7**, 1–13 (2017).
17. Zhang, N. *et al.* A handcuff model for the cohesin complex. *J. Cell Biol.* **183**, 1019 LP – 1031 (2008).
18. Eng, T., Guacci, V. & Koshland, D. Interallelic complementation provides functional evidence for cohesin-cohesin interactions on DNA. *Mol. Biol. Cell* **26**, 4224–4235 (2015).
19. Cattoglio, C. *et al.* Determining cellular CTCF and cohesin abundances to constrain 3D genome models. *Elife* **8**, (2019).

- 232 20. Capelson, M. & Corces, V. G. Boundary elements and nuclear organization. *Biol. cell* **96**, 617–  
233 29 (2004).
- 234 21. Walther, N. *et al.* A quantitative map of human Condensins provides new insights into mitotic  
235 chromosome architecture. *J. Cell Biol.* **217**, 2309–2328 (2018).
- 236 22. Ho, B., Baryshnikova, A. & Brown, G. W. Unification of Protein Abundance Datasets Yields a  
237 Quantitative *Saccharomyces cerevisiae* Proteome. *Cell Syst.* **6**, 192–205.e3 (2018).
- 238 23. Wang, B.-D., Eyre, D., Basrai, M., Lichten, M. & Strunnikov, A. Condensin Binding at  
239 Distinct and Specific Chromosomal Sites in the *Saccharomyces cerevisiae* Genome. *Mol. Cell.*  
240 *Biol.* **25**, 7216–7225 (2005).
- 241 24. Kschonsak, M. *et al.* Structural Basis for a Safety-Belt Mechanism That Anchors Condensin to  
242 Chromosomes. *Cell* **171**, 588–600.e24 (2017).
- 243 25. Brandão, H. B. *et al.* RNA polymerases as moving barriers to condensin loop extrusion. *Proc.*  
244 *Natl. Acad. Sci.* **116**, 20489–20499 (2019).
- 245 26. Stigler, J., Çamdere, G., Koshland, D. E. & Greene, E. C. Single-Molecule Imaging Reveals a  
246 Collapsed Conformational State for DNA-Bound Cohesin. *Cell Rep.* **15**, 988–998 (2016).
- 247 27. Goloborodko, A., Marko, J. F. & Mirny, L. A. Chromosome Compaction by Active Loop  
248 Extrusion. *Biophys. J.* **110**, 2162–2168 (2016).
- 249 28. Ganji, M., Kim, S. H., Van Der Torre, J., Abbondanzieri, E. & Dekker, C. Intercalation-based  
250 single-molecule fluorescence assay to study DNA supercoil dynamics. *Nano Lett.* **16**, 4699–  
251 4707 (2016).

252

253

# Figure legends

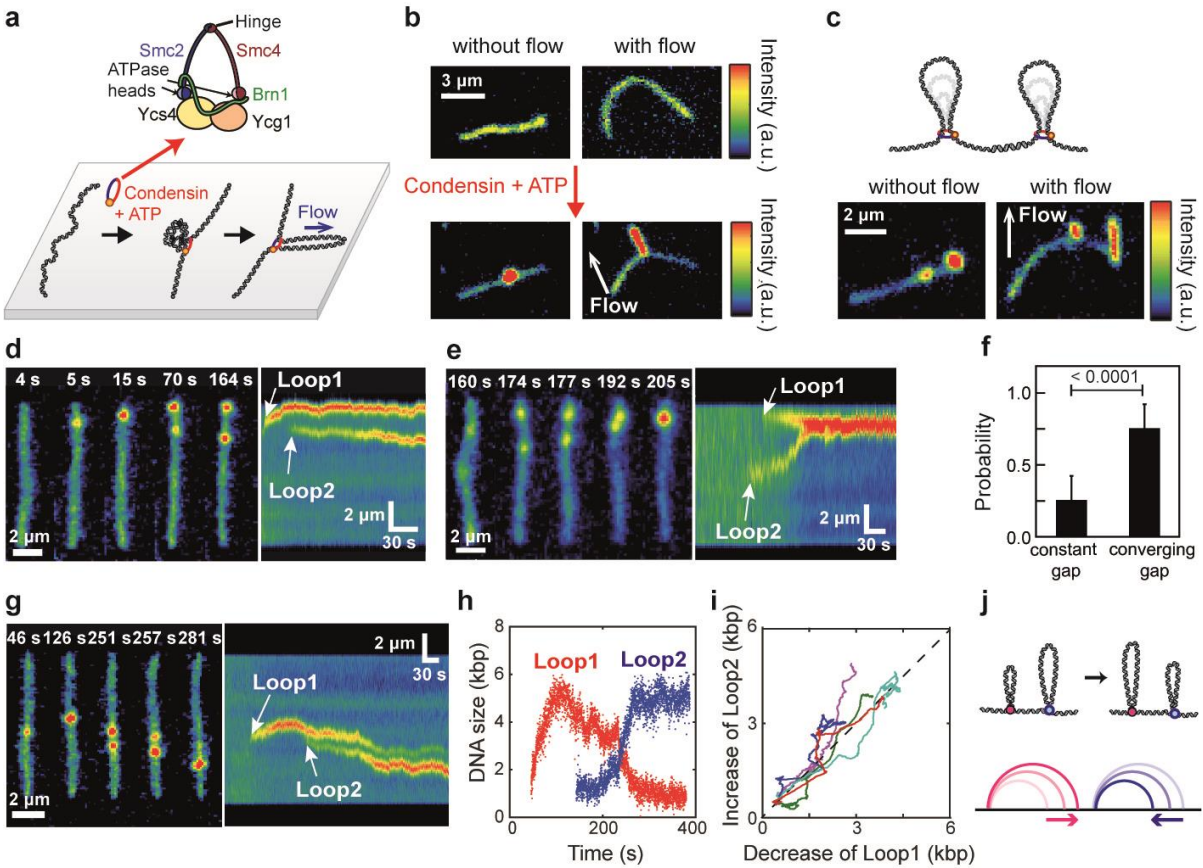


**Figure 1 | Interactions between multiple condensin-mediated DNA loops.**

**a**, Cartoon of the *S. cerevisiae* condensin featuring a large (~50 nm) ring structure (top), and schematic (bottom) and snapshots **b**, showing single-molecule visualizations of DNA loop extrusion on double-tethered SxO-stained DNA. Snapshots in (b) represent 21 independent experiments from 2 independently purified batches of condensin. **c**, Schematic and snapshots of two separate loops along a DNA molecule, representative of 14 independent experiments. Arrows in (b,c) indicate direction of buffer flow. **d**, **e**, Snapshots (left) and fluorescence-intensity kymographs (right) of two DNA loops that diverge (d) or converge (e). Representative of 16 independent experiments. **f**, Probability that two loops maintain a constant gap or mutually converge. Data shows the mean  $\pm$  95% confidence interval.  $P$ -value is determined by two-tailed student's t-test ( $n=32$  molecules, 11 independent experiments). **g**, Snapshots and kymograph showing the initial formation and shrinkage of a first loop (Loop 1) upon initiation of a second loop (Loop 2). **h**, Corresponding DNA size changes of the two loops in panel (g) versus time. (g-h) are representative of 16 independent experiments. **i**, Simultaneous change of DNA loop size for Loop2 versus for Loop1 ( $n=5$  molecules, 3 independent experiments, Extended data 1e for more examples). Dashed line has slope 1, indicating that Loop2 grows at the expense of a shrinkage of Loop1. **j**, Schematic diagram depicting DNA size exchange between two loops in real space (left) and in one-dimensional genomic space (right)<sup>14,27</sup>.

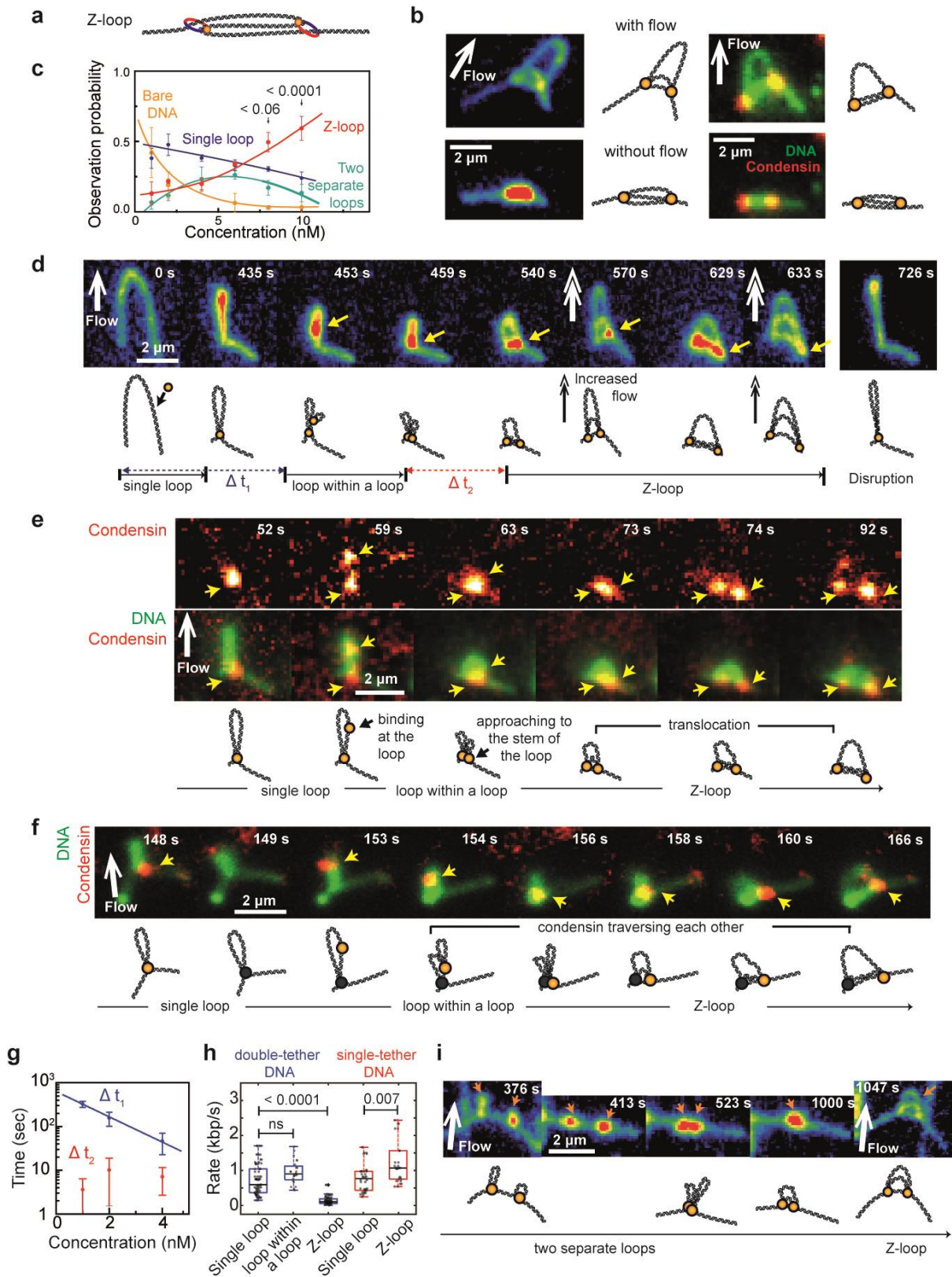


**Figure 2 | Condensins can traverse one another and form a Z-loop on DNA.**

**a**, Schematic of a Z-loop, which consists of three linearly stretched dsDNA molecules and two condensins, one located at each edge of the loop. **b**, Images of DNA (left) and overlaid images of DNA and condensin (right) revealing Z-loop by application of buffer flow. **c**, Probability of observing different DNA conformations versus condensin concentration. Data show mean $\pm$ SD from 4

independent experiments per concentration ( $n_{tot}=476$  molecules). Lines are guides to the eye. **d**, Snapshots showing DNA intermediates in Z-loop formation from bare DNA (0 s), to a single loop (435 s), to an additional loop within the initial loop (~459 s), to a Z-loop (633 s), and to disruption into a single loop (726 s). Yellow arrows denote the moving DNA parts. **e**, Snapshots of condensin (top), and overlaid images of DNA and condensin (bottom) showing locations of two condensins during Z-loop formation. **f**, Snapshots of overlaid images of DNA and condensin tracing the locations of the second condensin during Z-loop formation after the first condensin is photobleached (149s). Yellow arrows in (e,f) denote the locations of condensins. **g**, Waiting time  $\Delta t_1$  and  $\Delta t_2$  (defined in schematic in c) verses the protein concentrations. Line represents fit for  $\Delta t_1$  (coefficient of determination,  $R^2=0.998$ ). Its slope for  $\Delta t_1$  was significantly different from zero (slope= $-0.28\pm0.02$ ,  $P=0.03$ ) whereas that for  $\Delta t_2$  did not significantly differ from zero ( $R^2=0.335$ , slope= $0.07\pm0.09$ ,  $P=0.59$ ) (ANOVA test, significance set at  $P\leq0.05$ ). Data show mean $\pm$ SD.  $n=12, 11, 13$  molecules for 1, 2, 3 nM (20 independent experiments). **h**, DNA-loop extrusion rate for single loops, loops within a loop, and Z-loops estimated for single- and double-tethered DNA (Methods). The box plots span from 25 to 75% percentile, showing median as center line, and max. and min. values as whiskers. All  $P$  values determined by two-sided  $t$ -test. **i**, DNA snapshots showing a Z-loop formed by merging of two separate loops. Two individual loops initiated independently of each other and subsequently converged. After the merger (1000 s), they transformed into a Z-loop, which was visualized by the application of buffer flow (1047 s). Data in (b, d-f, i) represent 10, 20, 3, 10, 8 independent experiments, respectively. Schematic diagrams underneath the images in (b, d-f, i) provide visual guidance.



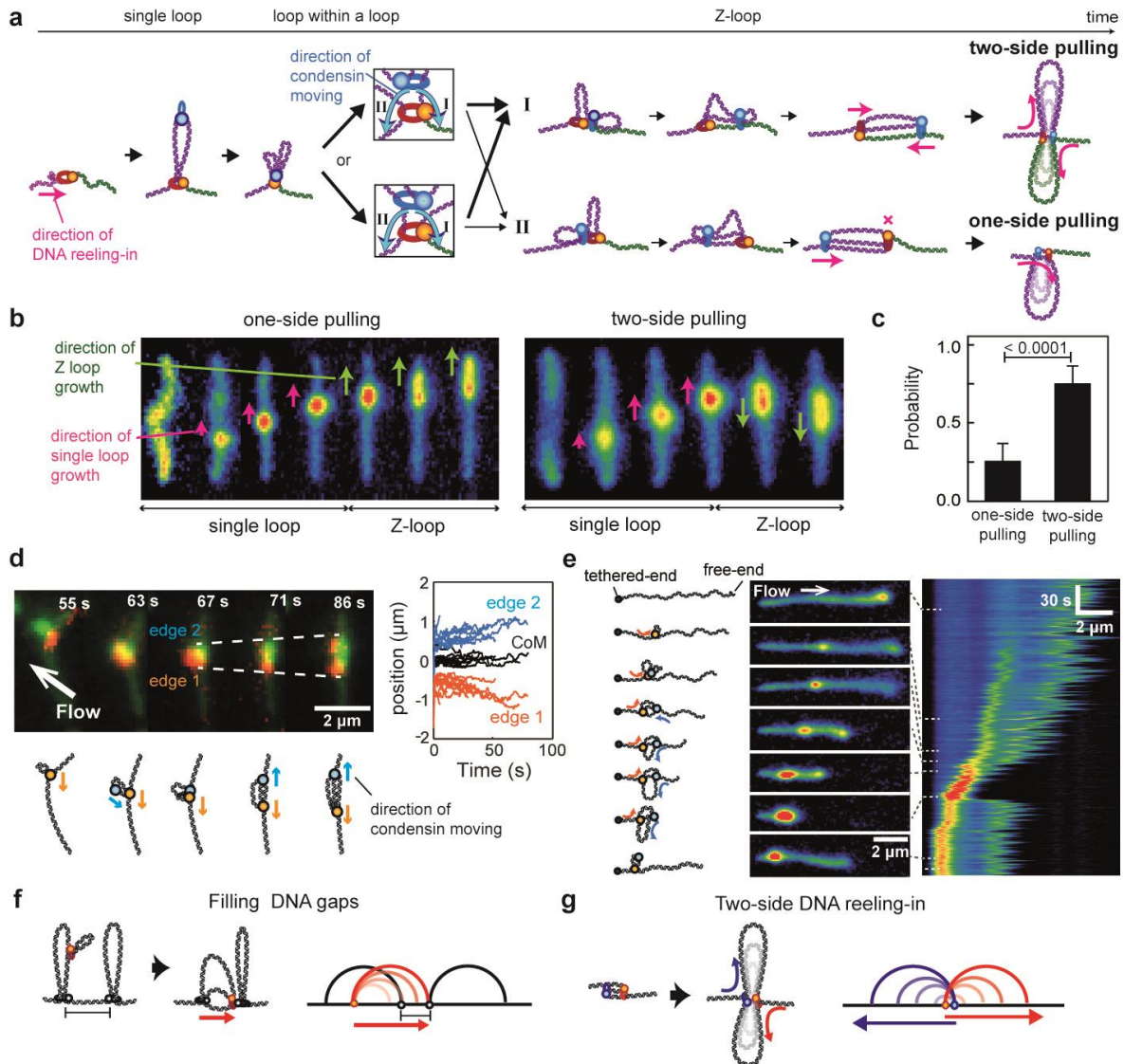


**Figure 3 | Possible impact of Z-loops on chromosomal compaction.**

**a**, Model of DNA Z-loop formation by two condensins. Depending on the orientations of the two condensins (zooms), the formed Z-loop can reel in DNA either from both sides of DNA (two-side pulling) or from one side (one-side pulling). **b**, Series of snapshots showing two DNA molecules where the initial single loop and the subsequent Z-loop grow from the same side of DNA (left) or from opposite sides (right). Representative of 12 independent experiments. **c**, Probability that a Z-loop pulls from one side or from two sides. Data shows the mean  $\pm$  95% confidence interval.  $P$  value is determined using two-tailed Student's  $t$ -test,  $n=70$  molecules from 12 independent experiments. **d**, Snapshots (top left) and schematics (bottom left) of overlay of SxO-stained DNA and ATTO647N-labeled condensin. For this molecule, binding of the second condensin occurred before the first condensin fully extruded the single loop, thus allowing for the first condensin to continue to reel in DNA during Z-loop extension. This results in a symmetric divergence of the two condensins. Simultaneous change of positions of two Z-loop edges (blue and orange) and of the center of mass (black) ( $n=11$  from 5 independent experiments; right). **e**, Schematics (left), snapshots (middle), and kymographs (right) of loop formation on a single-tethered DNA. Initially a single loop is formed, whereupon a two-side pulling Z-loop is formed, which is visualized in the broadening, accompanied by a simultaneous decrease in DNA length outside of the loop in both directions. At some point in time, the Z-loop disrupted and terminated into a single loop because the DNA that was reeled on the right reached the free end. Representative of 3 independent experiments. **f**, **g**, Schematic diagrams depicting possible implications of Z-loops for chromosomal compaction in real space (left) and 1D genomic space (right).

## Methods

### Condensin holocomplex purification

We used our previously published expression and purification protocols<sup>1</sup> to prepare the pentameric *S. cerevisiae* condensin complex.

### Fluorescent labeling of purified condensin complexes

The purified condensin complexes were fluorescently labeled as described previously<sup>1</sup>. Briefly, a 10 % excess of ATTO647N-maleimide (ATTO-TEC) was coupled to Coenzyme A (Sigma) in deoxygenated 100 mM sodium phosphate buffer at pH 7.00 for one hour at room temperature. 10 % equivalent of tris(2-carboxyethyl)phosphine was included halfway through the reaction and coupling was terminated with an excess of dithiothreitol. The reaction mixture was used for enzymatic covalent coupling to ybbR acceptor peptide sequences within the kleisin subunit in condensin holocomplexes (Brn1[13-24 ybbR, 3xTEV141]-His<sub>12</sub>-HA<sub>3</sub>; C5066), using a 5-fold excess of fluorophore to protein and ~1 μM Sfp synthase (NEB) for 16 hours at 6 °C in 50 mM TRIS-HCl pH 7.5, 200 mM NaCl, 5% v/v glycerol, 1 mM DTT, 0.01% Tween-20, 0.2 mM PMSF, 1 mM EDTA. Labeled protein was separated from unreacted fluorophore and the Sfp synthase by size-exclusion chromatography on a superose 6 3.2/200 (GE Healthcare) preequilibrated in 50 mM TRIS-HCl pH 7.5, 200 mM NaCl, 5% v/v glycerol, 1 mM MgCl<sub>2</sub>, 1 mM DTT).

### Double-tethered DNA assay for single-molecule imaging

Phage λ-DNA molecules were labelled with biotin at their both ends as described previously<sup>1</sup>. The biotinylated DNA molecules were introduced to the streptavidin-biotin-PEG coated glass surface of a flow cell at constant speed of 5 – 10 μL/min, resulting in attachment of DNA molecules with relative DNA extensions ranging from ~0.3 to ~0.6. The surface-attached DNA molecules were stained with 500 nM Sytox Orange (Invitrogen) intercalation dye and imaged in condensin buffer (50 mM TRIS-HCl pH 7.5, 50 mM NaCl, 2.5 mM MgCl<sub>2</sub>, 1 mM DTT, 5% (w/v) D-dextrose, 2 mM Trolox, 40 μg/mL glucose oxidase, 17 μg/mL catalase).

Real-time observation of multiple loop interactions by condensin was carried out by introducing condensin (1-10 nM) and ATP (5 mM) in the above specified condensin buffer. Although Z-loops were more frequently observed at higher concentrations (6-10 nM), most of the presented data were obtained in the concentration range of 2-4 nM. This was done to study single Z-loops and minimize measuring on DNA molecules that exhibited both a single loop and Z-loop simultaneously. For dual-color imaging of SxO-stained DNA and ATTO647N-labeled condensin, we also kept to this lower concentration range to minimize the background coming from both freely diffusing labelled condensin as well as from labelled condensins that transiently bound onto DNA without forming DNA loops.

Fluorescence imaging was achieved by using a home-built epi-fluorescence/TIRF microscopy. For imaging of SxO-stained DNA only, a 532-nm laser was used in epi-fluorescence mode. In the case of dual-color imaging, SxO-stained DNA and ATTO647N-labelled condensin were simultaneously imaged by alternating excitation of 532-nm and 640-nm lasers in Highly Inclined and Laminated Optical sheet (HILO) microscopy mode with a TIRF objective (Nikon). All images were acquired with an EMCCD camera (Ixon 897, Andor) with a frame rate of 10 Hz.

### Data analysis

#### *Estimation of condensin density per DNA length in the in vitro experiments*

Condensin density per DNA length was estimated as follows. First, movie frames were mapped into intensity profiles along the tether length by subpixel interpolation mapping. This was done for both the DNA and condensin signal channel. Next, these intensities were mapped in position versus time

kymographs. Condensin was counted by simple peak detection on the condensin profiles associated with each time point of the condensin kymograph. To suppress noise, the profiles were smoothened and only peaks above a threshold were counted. This threshold was taken as two times the standard deviation of the background noise. Next, we obtained the density of condensin per DNA length by summing the total number of detected condensin molecules over all time points, and dividing this by the total observed DNA length. To avoid biasing by surface effects, we excluded DNA tether lengths and condensin counts that were within ~400 nanometres of the tether attachment points. In this way, we obtained an average condensin density per tether. Finally, we repeated this measurement for ten separate tethers to find an average plus error for the condensin density.

For counting the number of molecules with two loops that were converging or kept a constant DNA gap in figure 1f, molecules exhibiting pronounced DNA slippage were excluded from the analysis.

#### *Estimation of the DNA size within and outside of loops*

To estimate the size of the DNA loops and the distance between loops, fluorescence intensity kymographs as shown in e.g. Fig. 1d were built from the intensity profiles of DNA molecules per time point as explained in our previous paper<sup>1</sup>. From the kymographs for individual molecules thus obtained, a loop analysis (cf. Figs. 1h, Extended Data Fig. 1, 2 etc.) was carried out as follows. The start center position and start time of a loop was indicated through user input. Then, the position of the loop at each time point was found by center-of-mass tracking over a section of the DNA molecule. This procedure was repeated until a user-set end time for this loop was reached. The data was stored as a position-time trace per loop.

For quantitation of the loop size, we define three regions per DNA molecule, namely 'Left', 'Middle', and 'Right', and collect the fluorescence intensities for the respective regions, viz., 'Left' as the intensity from the section left of the loop region, 'Middle' as the intensity of the DNA that is contained in the loop (Note that for Z-loops this includes the tether section below the loop region), and 'Right' as the intensity from the section right of the loop region. These three intensities were then expressed as percentages of the total intensity count, adding up to 100%. Using this intensity information, the sizes of the DNA loops (in kbp) were obtained by multiplication of the percentages by 48.5 kbp, yielding the size of individual single loops (e.g. Fig. 1h, Extended Data 1b,c) or the size of DNA within Z-loops (e.g. Extended Data Fig. 9f). For the detailed analysis for the estimation of DNA length in between two loops, we refer the readers to Extended Data Fig. 1a.

To obtain the observation frequencies in Fig. 2b, we performed 4 different experiments (i.e., in 4 different flow cells) per concentration. Per experiment, we counted the fraction of molecules (out of 11 to 40 molecules) that showed no loop/a single loop/two separate loops/a Z-loop for each frame, and divided that by the total number of molecules and by the number of frames. The error bars are the standard deviations from averaging the 4 different experiments.

#### *DNA-loop-extrusion rate estimation for single and Z-loop expansion*

To estimate the DNA-loop-extrusion rates of single and Z-loops in the absence of flow, we first built the intensity kymographs and extracted the time traces of DNA size changes in the loop region during single/Z-loop formation (e.g. Extended Data Fig. 9f). For the extraction of the respective rates, a linear fit to the increase of DNA amount during the first 10 seconds of the single/Z-loop growth was used.

#### *DNA-loop-extrusion rate estimation for a loop within a loop*

The rate of the DNA loop formation by the second condensin that docks within the DNA loop previously formed by a first condensin was estimated in the presence of buffer flow, as the change from a single loop to a nested loop can only be seen by flow-induced DNA stretching. For this, we built the intensity kymographs along the axis parallel to the extruded single loop (e.g. Extended Data 9b). From these kymographs, the rate of loop within a loop formation was determined by the change in the physical length of the single loop and that of nested loop, divided by the time duration of the formation process of the second loop.



432 *DNA-loop-extrusion rate estimation for single and Z-loop growth for single tethered DNA*  
433 The rate of single and Z-loop growth for single-tethered DNA was estimated from the change of the  
434 DNA end-to-end length divided by the time duration.

435  
436  
437  
438